

# Methanol-steam reforming over a ZnO–Cr<sub>2</sub>O<sub>3</sub>/CeO<sub>2</sub>–ZrO<sub>2</sub>/Al<sub>2</sub>O<sub>3</sub> catalyst

Weiqliang Cao<sup>a,b</sup>, Guangwen Chen<sup>a,\*</sup>, Shulian Li<sup>a</sup>, Quan Yuan<sup>a</sup>

<sup>a</sup> Dalian Institute of Chemical Physics, Chinese Academy of Sciences, 457 Zhongshan Road, Dalian 116023, China

<sup>b</sup> Graduate School of the Chinese Academy of Sciences, Beijing 100039, China

Received 26 December 2005; received in revised form 3 March 2006; accepted 13 March 2006

## Abstract

This study showed that a ZnO–Cr<sub>2</sub>O<sub>3</sub>/CeO<sub>2</sub>–ZrO<sub>2</sub>/Al<sub>2</sub>O<sub>3</sub> (Zn–Cr) catalyst was a promising catalyst for hydrogen production from methanol due to its high stability and selectivity. There was no significant deactivation of the catalyst over 300 min of continuous operation when water was introduced into the feed. In the absence of water, the catalyst deactivated rapidly due to coke formation. The addition of water into the feed changed the route of methanol conversion and improved its rate. In order to investigate the pathway of CO formation, three reactions, i.e. decomposition of methanol (DM), steam reforming of methanol (SRM) and water gas-shift (WGS), were studied in this paper. The results showed that CO and CO<sub>2</sub> were produced through the DM reaction and SRM reaction, respectively. The WGS and reverse WGS reactions were negligible. Adding H<sub>2</sub> and CO in the feed did not influence the process behavior of the SRM reaction. The addition of CO<sub>2</sub> and H<sub>2</sub>O into the feed decreased the yield of CO<sub>2</sub>. © 2006 Elsevier B.V. All rights reserved.

**Keywords:** Methanol-steam reforming; Water gas-shift; Decomposition of methanol; Microchannel reactor; CO formation; ZnO–Cr<sub>2</sub>O<sub>3</sub>/CeO<sub>2</sub>–ZrO<sub>2</sub>/Al<sub>2</sub>O<sub>3</sub> catalyst

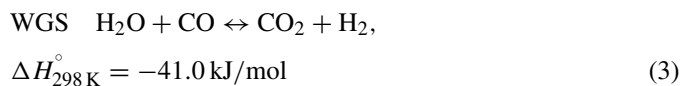
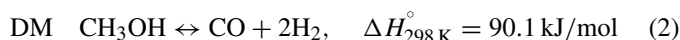
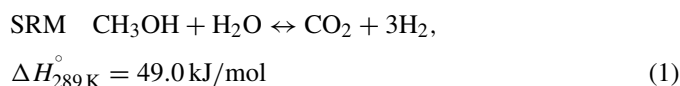
## 1. Introduction

Fuel cells are expected to play a major role in the future for their high efficiency and low emission of pollution. However, the storage and handling of on-board hydrogen in the fuel cell vehicles is still an unsolved issue. One of the solutions is to use hydrocarbon fuels as hydrogen carrier. Among all possible choices of fuels, methanol is considered to be the most favorable candidate due to its high ratio of hydrogen to carbon and low reaction temperatures [1].

The current investigation of hydrogen production from methanol mainly focuses on Cu-based and Pd–Zn catalysts [2–8]. However, Cu-based catalysts deactivate quickly and Pd–Zn catalysts are extremely expensive, though they have a high activity and selectivity. Therefore, they are not suitable for on-board production of hydrogen. It is well known that ZnO–Cr<sub>2</sub>O<sub>3</sub> catalysts have been used for hydrocarbon synthesis from synthesis gas [9,10]. Our studies show that ZnO–Cr<sub>2</sub>O<sub>3</sub> catalysts are promising catalysts for the hydrogen production from methanol. However, CO is formed inevitably in the reaction process, which has the largest influence on the performance of proton exchange membrane fuel cells (PEMFCs) [11]. Although

there are numerous investigations of CO formation over Cu-based [4,12–15] and Pd–Zn [7] catalysts, the route of CO formation on the Zn–Cr catalysts is still not clearly understood. In order to inhibit the formation of CO in the steam reforming process, it is crucial to investigate the route of CO formation.

Peppley et al. thought that the following three reactions should be included in the reaction scheme of methanol-steam reforming over a Cu/ZnO/Al<sub>2</sub>O<sub>3</sub> catalyst:



Previous literature on the reaction mechanisms of SRM with respect to the formation of CO suggested that CO was produced mainly through three pathways: (1) CO is an intermediate and formed directly through the DM reaction followed by the WGS reaction [13,16–18]. (2) CO is released by the RWGS reaction as a secondary product [4,12,19–21]. In addition, (3) CO is produced directly from the DM reaction without significant WGS reaction [22,23].

\* Corresponding author. Tel.: +86 411 437 9031; fax: +86 411 469 1570.  
E-mail address: gwchen@dicp.ac.cn (G. Chen).

Generally, steam reforming was conducted in a conventional fixed bed reactor heated in a furnace. However, one of the most significant drawbacks in such experiments is the nonisothermality of the catalytic bed caused by the endothermic SRM reaction. For strongly endothermic chemical reactions, the cold spots in the packed catalyst bed usually result in underestimation of the catalyst activity. Microchannel reactors are able to offer an isothermal environment because of the reduction of the channel sizes [2]. The narrow radial distance leads to a short contact time of reactants. This short contact time not only avoids the formation of unwanted by-products, but also allows a quick response to dynamic changes in the inlet conditions. Recently, microchannel reactors have been chosen to investigate the steam reforming of methanol by some researchers [2–6]. However, it is difficult to introduce the catalyst into the microchannels, because the catalyst layers can prevent the bonding process or the bonding process can destroy the catalysts. In this paper, the screened catalyst particles were directly introduced into the microchannels.

In this work, we first investigated the performance of a Zn–Cr catalyst for methanol-steam reforming, and then tried to clarify the reaction and in particular the route of CO formation. In a subsequent publication, we will determine the exact rate-expression of methanol-steam reforming.

## 2. Experimental

### 2.1. Catalyst preparation

The Zn–Cr catalyst supported on treated  $\gamma$ - $\text{Al}_2\text{O}_3$  was prepared by a co-impregnation method. The  $\gamma$ - $\text{Al}_2\text{O}_3$  was first impregnated by nitric acid solution of  $\text{Ce}(\text{NO}_3)_2 \cdot 6\text{H}_2\text{O}$  and  $\text{Zr}(\text{NO}_3)_3$  (Ce:Zr = 4:1, Shanghai Yuelong Chemical Company).

The impregnated sample was then dried in air and calcined at  $500^\circ\text{C}$  for 4 h. The calcined sample was further impregnated by nitric acid solution of  $\text{Zn}(\text{NO}_3)_2 \cdot 6\text{H}_2\text{O}$  and  $\text{Cr}(\text{NO}_3)_3 \cdot 9\text{H}_2\text{O}$  (Zn:Cr = 2:1, Shanghai Chemical Company) and was then dried in air. The  $\text{ZnO-Cr}_2\text{O}_3/\text{CeO}_2\text{-ZrO}_2/\text{Al}_2\text{O}_3$  sample was finally calcined at  $500^\circ\text{C}$  for 4 h. The loadings of the Ce–Zr and Zn–Cr coatings were 25 and 15 wt.%, respectively. The prepared sample was pelletized and sieved (0.3–0.45 mm) for the experiments.

### 2.2. Reactor and catalytic activity

A microchannel reactor, made of stainless steel, was used to keep isothermal conditions in the catalyst bed (Fig. 1). The reactor consisted of one chip and two cover sheets and was sealed with a graphite sheet. The plate had 30 parallel channels (1 mm wide, 1.2 mm deep and 30 mm long) which contained 1.195 g catalyst.

A schematic sketch of the testing system setup is shown in Fig. 2. All gases (>99.99% purity), including the balance gas ( $\text{N}_2$ ), were precisely controlled and delivered into the vaporizer by mass flow controllers. The liquid methanol (>99.5% purity) and water mixture was pumped into the vaporizer with a precise P230 constant flow pump (Dalian Elite Analytical Instruments Company). The reactants were vaporized and preheated to a defined temperature in the vaporizer, and subsequently reacted in the reactor. The reactor effluent passed through a cold trap and the dry gaseous products were analyzed on-line by a gas chromatograph (GC4000A, Beijing East & West Analytical Instruments Inc.) equipped with a thermal conductivity detector (TCD). A carbon molecular sieve column was used to analyze the dry gaseous components. The flow rate of the dry gaseous products was measured by a soap bubble flow meter.

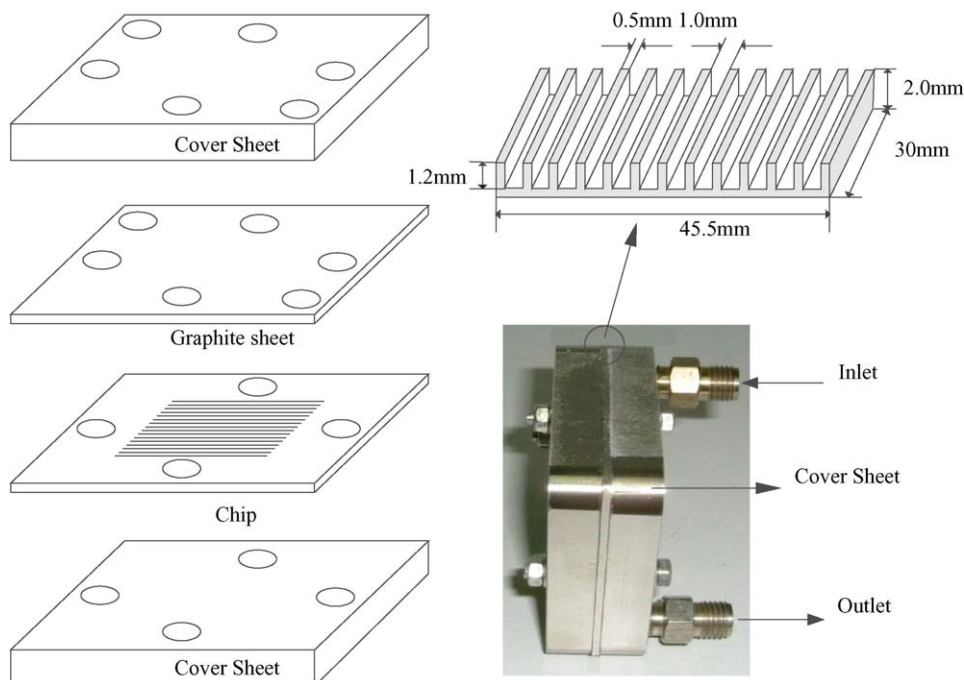


Fig. 1. Schematic diagram of the microchannel reactor structure.

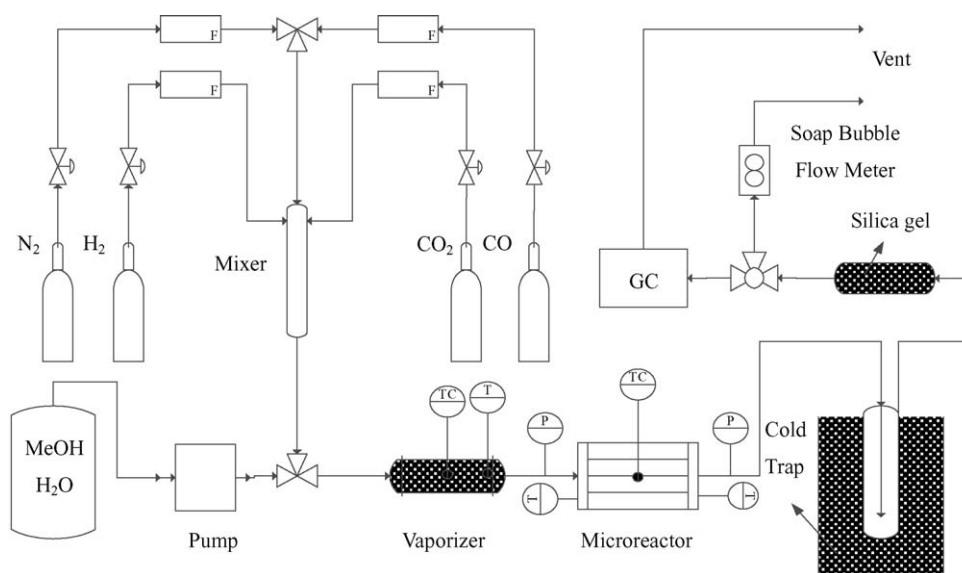


Fig. 2. Schematic sketch of the testing system setup.

In this paper, the gas hourly space velocity (GHSV) is defined as the feed flow rate per total reactor volume, and the  $\text{CO}/(\text{CO} + \text{CO}_2)$  ratio in the product is referred to as CO selectivity. The methanol conversion and product yields are calculated based on the flow rate and compositions of the dry gaseous products. CO and  $\text{CO}_2$  yields are defined as the molar ratio of CO and  $\text{CO}_2$  produced to methanol in the feed, respectively. All the data were collected when the catalytic activity was kept stable, and the material balances on  $\text{N}_2$  were calculated to verify the measurement accuracy.

### 3. Results and discussion

#### 3.1. Activity for SRM

The steam-to-carbon molar ratio and GHSV in this particular run were 1.4 and  $25\,000\text{ h}^{-1}$ , respectively. Fig. 3 shows the effect of reaction temperature on the methanol conversion and product distribution over the catalyst. The methanol conversion exhibited the typical S-shaped temperature dependence. The ratio of  $\text{H}_2$  and  $\text{CO}_2$  remained approximately 3:1 in the whole temperature range. CO was the main by-product formed

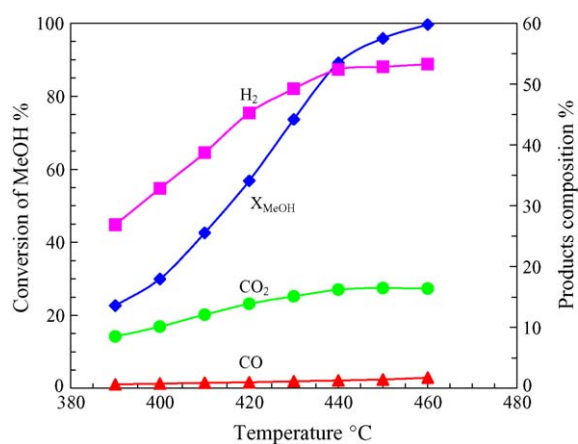


Fig. 3. Methanol conversion and product distribution for steam reforming vs. reaction temperature (GHSV =  $25\,000\text{ h}^{-1}$ , the methanol and the water contents in feed were 25 and 35 mol%, respectively).

in the reforming process, but its concentration was far lower than the balanced stoichiometric concentration of the WGS showing that CO cannot be a reaction intermediate. These results were in quite good agreement with that obtained on Cu-based

Table 1  
SRM, WGS and RWGS on the Zn–Cr catalyst

Reaction	Reaction condition		Outlet composition (%)		
	$T$ (°C)	Inlet composition	$\text{CO}_2$	CO	$\text{H}_2$
SRM	410	25% MeOH, 35% $\text{H}_2\text{O}$ , 40% $\text{N}_2$	12.08	0.89	38.73
WGS		12.5% CO, 30% $\text{H}_2\text{O}$ , 57.5% $\text{N}_2$	0.82	14.67	0.81
RWGS		15% $\text{CO}_2$ , 40% $\text{H}_2$ , 45% $\text{N}_2$	14.20	0.83	39.84
SRM	430	25% MeOH, 35% $\text{H}_2\text{O}$ , 40% $\text{N}_2$	15.12	1.15	49.20
WGS		15% CO, 30% $\text{H}_2\text{O}$ , 55% $\text{N}_2$	1.29	17.33	1.30
RWGS		20% $\text{CO}_2$ , 60% $\text{H}_2$ , 20% $\text{N}_2$	18.20	1.28	60.91
RM	450	25% MeOH, 35% $\text{H}_2\text{O}$ , 40% $\text{N}_2$	16.50	1.46	52.84
WGS		15% CO, 30% $\text{H}_2\text{O}$ , 55% $\text{N}_2$	1.85	16.51	1.83
RWGS		20% $\text{CO}_2$ , 60% $\text{H}_2$ , 20% $\text{N}_2$	17.30	1.83	61.14

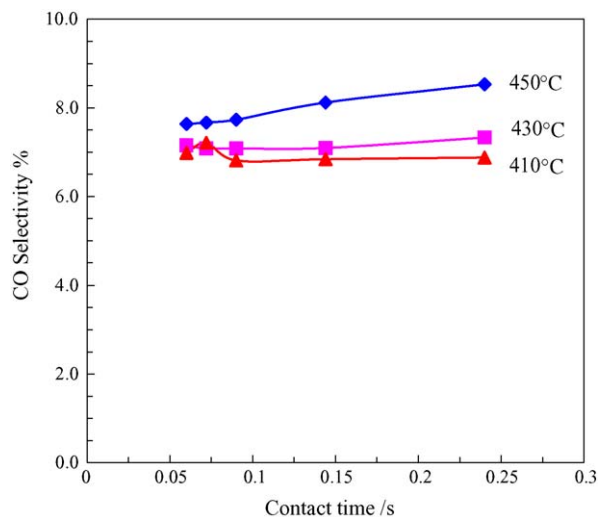


Fig. 4. CO selectivity as a function of contact time at different temperatures.

catalysts. However, the Zn–Cr catalyst needed a higher reaction temperature to acquire 100% conversion than Cu-based catalysts [2,4,24]. A temperature greater than 460 °C was needed to obtain 100% conversion at the GHSV of 25 000 h<sup>-1</sup>.

### 3.2. CO formation in SRM

In order to investigate the pathway of CO production in the steam reforming three reactions, i.e. SRM, WGS and RWGS, were investigated on the catalyst. The conditions and results of these reactions were showed in Table 1. The WGS reaction was first conducted under the reaction conditions similar to the outlet composition of the steam reforming based on the assumption that the CO<sub>2</sub> in the steam reforming was produced through WGS. However, the CO composition after WGS was much greater than that of the steam reforming process, which showed that CO<sub>2</sub> could not be formed through CO in SRM. Therefore the WGS reaction in the reforming process can be neglected due to its low conversion.

However, it cannot be judged whether CO is formed through RWGS because the CO<sub>2</sub> outlet composition of RWGS is quite close to that of SRM. In order to clarify whether CO is produced through the RWGS reaction, the SRM reaction with different contact time was performed on the catalyst. Fig. 4 shows a plot of CO selectivity versus contact time at different temperatures. The CO selectivity first declined gradually with decreasing reaction time and then approached a constant level when the contact time was less than 0.09 s. This result showed that CO was not a secondary product formed through CO<sub>2</sub>. Therefore the RWGS reaction could be ignored in the reforming process.

In addition, the influence of H<sub>2</sub> on SRM, DM and RWGS was investigated at 450 °C and the results are plotted in Fig. 5. The CO concentration reduced slowly from 1.49 to 1.29% at 450 °C when the H<sub>2</sub> concentration varied between 0 and 40%. The methanol conversion kept constant throughout the H<sub>2</sub> concentration range (Fig. 5a). A similar result could be gotten in the DM reaction (Fig. 5c). However, increasing H<sub>2</sub> caused the CO

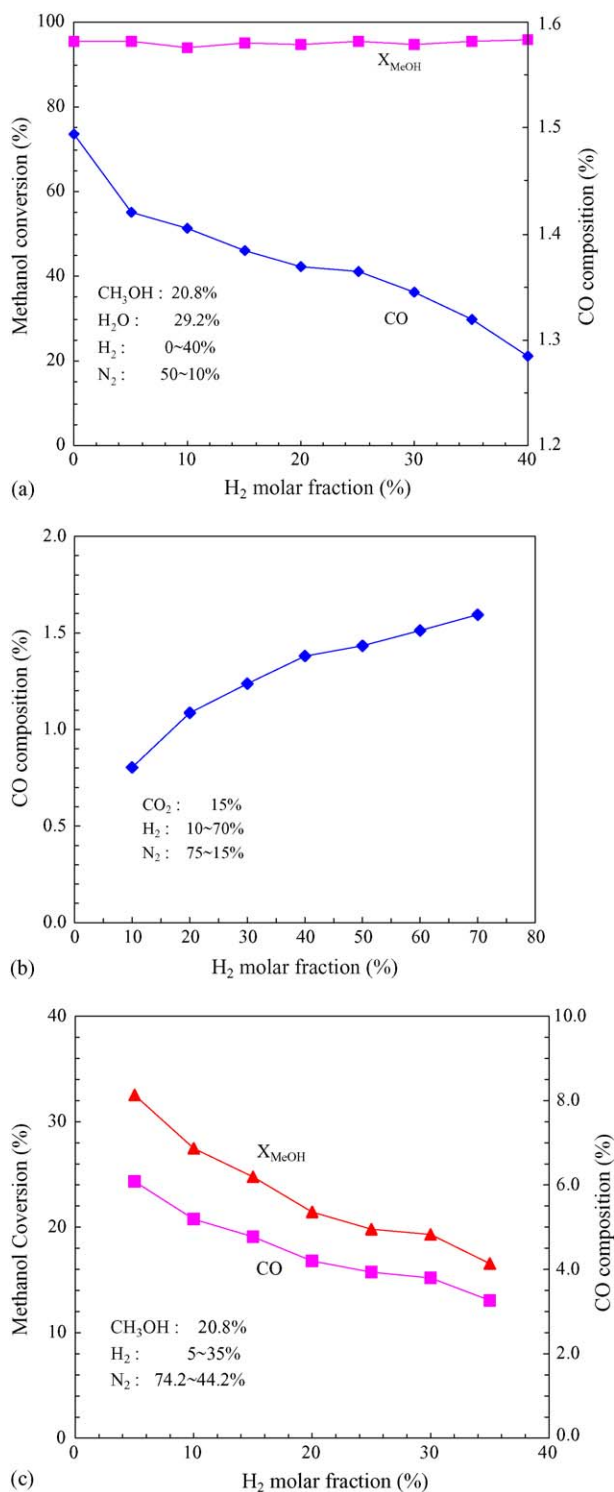


Fig. 5. Effect of H<sub>2</sub> on the SRM reaction (a), the reverse WGS reaction (b) and the DM reaction (c) at 450 °C (GHSV = 36 000 h<sup>-1</sup>).

concentration to increase according to the reverse WGS reaction (Fig. 5b). The CO composition increased gradually from 0.8 to 1.59% in the reverse WGS reaction when the H<sub>2</sub> concentration was increased from 10 to 70%. These results further proved that the CO in the steam reforming is mainly produced through the DM reaction without the WGS reaction.

### 3.3. Stability for DM and SRM

The catalyst stability in the DM and SRM was evaluated for 300 min using the same methanol inlet content and the reaction conditions were kept constant ( $T=440\text{ }^{\circ}\text{C}$ ,  $\text{GHSV}=25\,000\text{ h}^{-1}$ ). Fig. 6 indicates the stability of the Zn–Cr catalyst for DM and SRM. In the presence of water, the Zn–Cr catalyst showed a higher thermal stability than Cu-based catalysts. One of the most important reasons is probably that the thermal resistance of  $\text{ZnO-Cr}_2\text{O}_3$  is superior to that of Cu which easily sinters at high temperatures. Studies have shown that the introduction of  $\text{ZrO}_2$  into the ceria lattice significantly increases the oxygen species storage capacity [25–29] and thermal resistance [30–33] due to the formation of a solid solution. Additionally, the results reported by Agrell et al. [24] showed that catalysts containing  $\text{ZrO}_2/\text{Al}_2\text{O}_3$  were highly resistant to redox cycles and exhibit high stability. These factors probably helped to improve the stability of the catalyst.

In the absence of water, the activity of the Zn–Cr catalyst decreased rapidly and the catalyst had a significant weight increase (5.3%, excluding moisture) caused most likely by car-

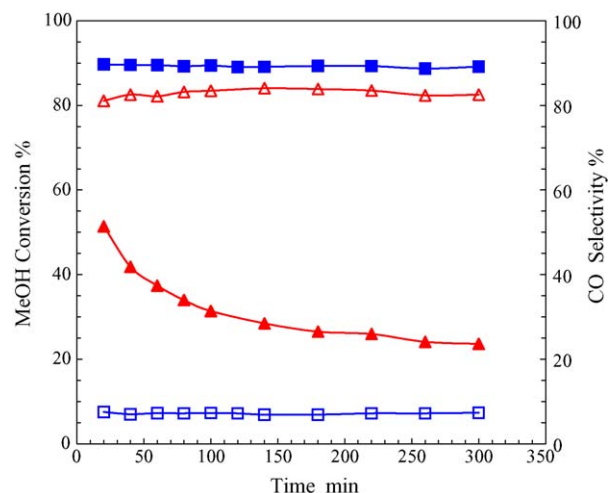


Fig. 6. Variation of methanol conversion (solid symbol) and CO selectivity (open symbol) with reaction time on DM ( $\Delta$ ,  $\blacktriangle$ ) and SRM ( $\square$ ,  $\blacksquare$ ) ( $T=440\text{ }^{\circ}\text{C}$ ,  $\text{GHSV}=25\,000\text{ h}^{-1}$ ).

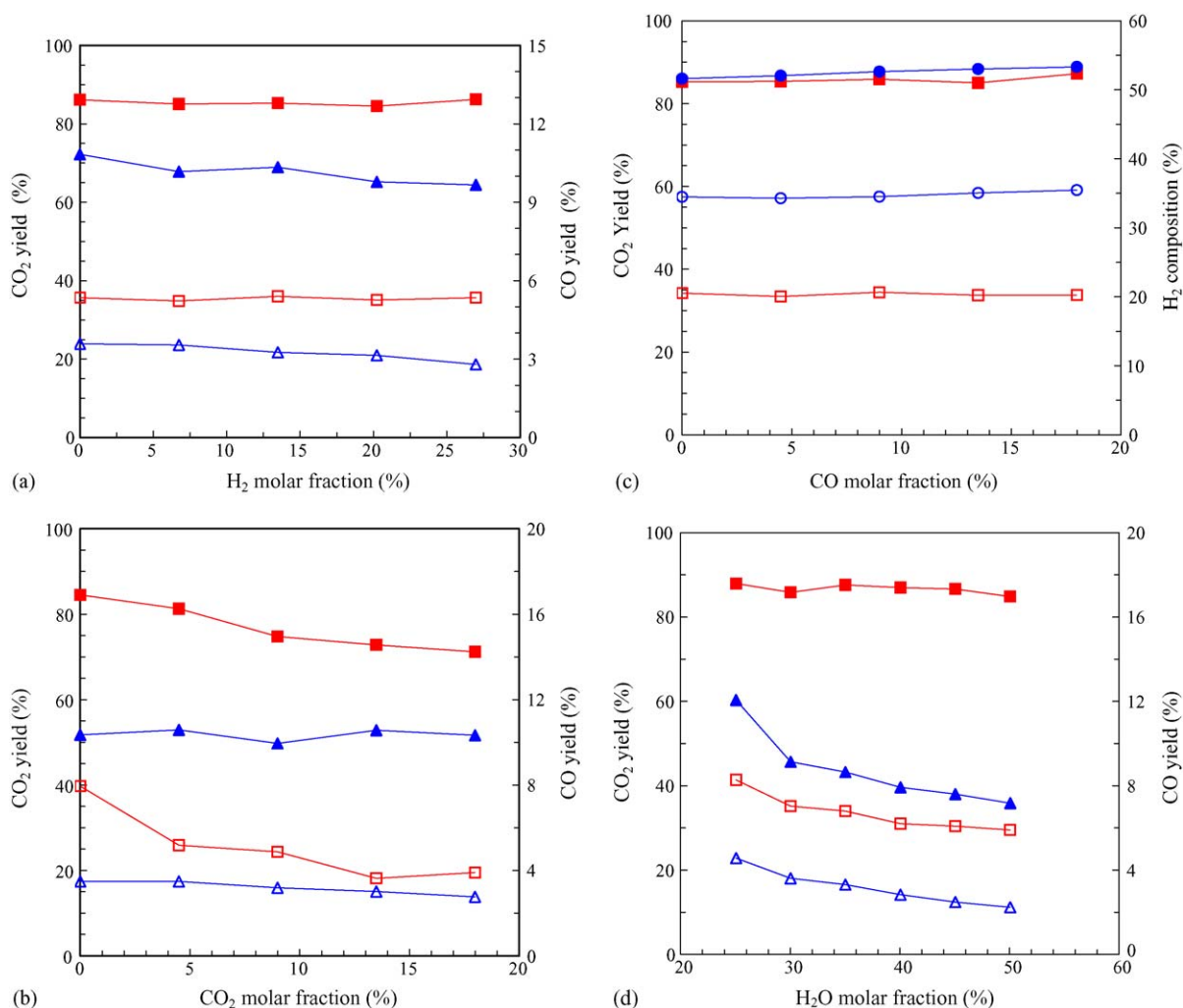


Fig. 7. Effect of  $\text{H}_2$  (a),  $\text{CO}_2$  (b),  $\text{CO}$  (c) and  $\text{H}_2\text{O}$  (d) on the SRM reaction at  $410\text{ }^{\circ}\text{C}$  (open symbol) and  $450\text{ }^{\circ}\text{C}$  (solid symbol): ( $\square$ ,  $\blacksquare$ )  $\text{CO}_2$ , ( $\Delta$ ,  $\blacktriangle$ )  $\text{CO}$ , ( $\circ$ ,  $\bullet$ )  $\text{H}_2$  ( $\text{GHSV}=25\,000\text{ h}^{-1}$ ).

bon fouling. Additionally, the initial conversion of methanol decomposition was lower than that of steam reforming. It could be inferred that different reactions occurred on the catalyst when water was introduced into the feed.

### 3.4. Influence of gaseous products and water on SRM

Different concentrations of gaseous products were introduced into the reactant mixtures of methanol and water, and N<sub>2</sub> was used as a balance gas to keep the contact time constant. Diffusive limitations were excluded in this particular run. Fig. 7 shows the influences of product gases and water on the steam reforming at different temperatures. Increasing the inlet content of H<sub>2</sub> could hardly vary the CO<sub>2</sub> yield showing that H<sub>2</sub> had little influence on the SRM reaction over the Zn–Cr catalyst, though H<sub>2</sub> had a negative influence over Cu-based catalysts [34,35]. But adding H<sub>2</sub> slightly reduced the CO yield, and thus H<sub>2</sub> decreased the rate of the DM reaction. Co-feeding of CO<sub>2</sub> reduced the yield of CO<sub>2</sub> significantly showing that CO<sub>2</sub> suppressed the SRM reaction. The influences of CO on the SRM reaction are negligible. In addition, excess water led to declining CO<sub>2</sub> and CO yields, which showed that water suppressed the SRM and DM reactions.

## 4. Conclusion

The Zn–Cr catalyst is a potential catalyst for methanol-steam reforming due to its high thermal stability, though it needs a higher reaction temperature to equal the conversion of Cu-based and Pd-based catalysts. CO<sub>2</sub> and H<sub>2</sub> are produced mainly through the SRM reaction and CO is formed mainly through the DM reaction. Both the WGS and RWGS reactions can be ignored. In the absence of water, there is a rapid deactivation of the catalyst caused by coking.

## Acknowledgements

We gratefully acknowledge the financial supports for this project from National Natural Science Foundation of China and China National Petroleum Corporation (Nos. 20176057, 20122201 and 20490200), Key Program for International Cooperation of Science and Technology (No. 2001CB711203) and Innovative Fund of Dalian Institute of Chemical Physics, Chinese Academy of Sciences (No. K2003E2).

## References

[1] B. Lindström, L.J. Pettersson, *Int. J. Hydrogen Energy* 26 (2005) 923–933.  
 [2] C. Cao, G. Xia, J. Holladay, E. Jones, Y. Wang, *Appl. Catal. A* 262 (2004) 19–29.

[3] P. Pfeifer, K. Schubert, G. Emig, *Appl. Catal. A* 286 (2005) 175–185.  
 [4] H. Purnama, T. Ressler, R.E. Jentoft, H. Soerijanto, R. Schlögl, R. Schomäcker, *Appl. Catal. A* 259 (2004) 83–94.  
 [5] X.H. Yu, S.T. Tu, Z.D. Wang, Y.S. Qi, *J. Power Sources* 12 (2005) 345–348.  
 [6] G.W. Chen, Q. Yuan, S.L. Li, *Chin. J. Catal.* 23 (2002) 491–492.  
 [7] S. Liu, K. Takahashi, K. Uematsu, M. Ayabe, *Appl. Catal. A: Gen.* 283 (2005) 125–135.  
 [8] S.L. Li, G.W. Chen, F.J. Jiao, H.Q. Li, *Chin. J. Catal.* 25 (2004) 979–982.  
 [9] F. Simard, U.A. Sedran, J. Sepúlveda, N.S. Fígoli, H.I. de Lasa, *Appl. Catal. A* 125 (1995) 81–98.  
 [10] M.C.J. Bradford, M.V. Konduru, D.X. Fuentes, *Fuel Proc. Tech.* 83 (2003) 11–25.  
 [11] K. Narusawa, M. Hayashida, Y. Kamiya, H. Roppongi, D. Kurashima, K. Wakabayashi, *JSAE Rev.* 24 (2003) 41–46.  
 [12] J. Agrell, H. Birgersson, M. Boutonnet, *J. Power Sources* 106 (2002) 249–257.  
 [13] J.C. Amphlett, M.J. Evans, R.F. Mann, R.D. Weir, *Can. J. Chem. Eng.* 63 (1985) 605–611.  
 [14] B.A. Peppley, J.C. Amphlett, L.M. Kearns, R.F. Mann, *Appl. Catal. A* 179 (1999) 21–29.  
 [15] B.A. Peppley, J.C. Amphlett, L.M. Kearns, R.F. Mann, *Appl. Catal. A* 179 (1999) 31–49.  
 [16] J. Barton, V. Pour, *Coll. Czech. Chem. Commun.* 45 (1980) 3402.  
 [17] E. Santacesaria, S. Carra, *Appl. Catal.* 5 (1983) 345.  
 [18] R. Peters, H.G. Düsterwald, B. Hühlein, *J. Power Sources* 86 (2000) 507–514.  
 [19] J.P. Breen, J.R.H. Ross, *Catal. Today* 51 (1999) 521–533.  
 [20] J.K. Lee, J.B. Ko, D.H. Kom, *Appl. Catal. A* 278 (2004) 25–35.  
 [21] K. Geissler, E. Newson, F. Vogel, T.B. Truong, P. Hottinger, A. Wokaum, *Phys. Chem. Chem. Phys.* 3 (2001) 289.  
 [22] I.A. Fisher, A.T. Bell, *J. Catal.* 184 (1999) 357–376.  
 [23] D. Bianchi, T. Chafik, M. Khalifallah, S.J. Teichner, *Appl. Catal. A* 123 (1995) 89–110.  
 [24] J. Agrell, H. Birgersson, M. Boutonnet, I. Melián-Cabrera, R.M. Navarro, J.L.G. Fierro, *J. Catal.* 219 (2003) 389–403.  
 [25] C.E. Hori, H. Permana, K.Y.S. Ng, A. Brenner, K. More, K.M. Rahmoeller, D. Belton, *Appl. Catal. B* 16 (1998) 105–117.  
 [26] P. Fornasiero, G. Balducci, R. Di Monte, J. Kašpar, V. Sergo, G. Gubitosa, A. Ferrero, M. Graziani, *J. Catal.* 164 (1996) 173–183.  
 [27] H. Vidal, S. Bernal, J. Kašpar, M. Pijolat, V. Perrichon, G. Blanco, J.M. Pintado, R.T. Baker, G. Colon, F. Fally, *Catal. Today* 54 (1999) 93–100.  
 [28] G. Vlaic, R. Di Monte, P. Fornasiero, E. Fonda, J. Kašpar, M. Graziani, *J. Catal.* 182 (1999) 378–389.  
 [29] P. Fornasiero, E. Fonda, R. Di Monte, G. Vlaic, J. Kašpar, M. Graziani, *J. Catal.* 187 (1999) 177–185.  
 [30] F. Fally, V. Perrichon, H. Vidal, J. Kaspar, G. Blanco, J.M. Pintado, S. Bernal, G. Colon, M. Daturi, J.C. Lavalley, *Catal. Today* 59 (2000) 373–386.  
 [31] P. Fornasiero, G. Balducci, J. Kašpar, S. Meriani, R. Di Monte, M. Graziani, *Catal. Today* 29 (1996) 47–52.  
 [32] X.D. Wu, B. Yang, D. Weng, *J. Alloys Comp.* 376 (2004) 241–245.  
 [33] S.L. Li, G.W. Chen, J.L. Sun, H.Q. Li, *Chin. J. Catal.* 23 (2002) 341–344.  
 [34] C.J. Jiang, D.L. Trimm, M.S. Wainwright, N.W. Cant, *Appl. Catal. A* 93 (1993) 245–255.  
 [35] C.J. Jiang, D.L. Trimm, M.S. Wainwright, N.W. Cant, *Appl. Catal. A* 97 (1993) 145–158.